Journal of The Electrochemical Society, **147** (6) 2312-2318 (2000)
S0013-4651(99)07-002-0 CCC: $7.00

Integrity of Copper-Tantalum Nitride Metallization under Different Ambient Conditions

K. P. Yap,[a,b,c,z] H. Gong,[a] J. Y. Dai,[b] T. Osipowicz,[d] L. H. Chan,[c] and S. K. Lahiri[b,*]

[a]*Department of Materials Science, Faculty of Science, National University of Singapore, Singapore 119260*
[b]*Institute of Materials Research and Engineering, Singapore 119260*
[c]*Chartered Semiconductor Manufacturing Limited, Singapore 738406*
[d]*Department of Physics, Faculty of Science, National University of Singapore, Singapore 119260*

The integrity of the Cu/IMP $Ta_{2.3}N$ metallization under different annealing ambients has been investigated by Rutherford backscattering spectrometry (RBS), transmission electron microscopy (TEM), X-ray diffractometry (XRD), Auger electron spectroscopy, scanning electron microscopy, and atomic force microscopy techniques. Results from XRD and TEM show that the as-deposited amorphous $Ta_{2.3}N$ barrier crystallizes upon annealing at 500°C, forming a Ta_2N crystalline phase. The sheet resistance of Cu/$Ta_{2.3}N$ metallization remains unchanged upon annealing in Ar or N_2 up to 750°C. No observable interdiffusion was detected by RBS upon annealing at temperatures below 500°C in Ar or N_2. However, above 500°C, the integrity of Cu/$Ta_{2.3}N$ metallization begins to degrade due to out-diffusion of a small amount of Ta into Cu. On the other hand, in an N_2/20% O_2 ambient, the sheet resistance of the metallization is found to increase drastically upon annealing at a temperature above 200°C, an observation that has been attributed to the formation of porous Cu oxide layer. Delamination of Cu oxide from oxide/barrier interface occurs at 400°C. The result highlights the importance of isolating Cu/$Ta_{2.3}N$ metallization from oxygen exposure during back end processing.

Manuscript submitted July 1, 1999; revised manuscript received January 28, 2000.

The major reasons for replacing aluminum (Al) metallization with copper (Cu) metallization for deep submicrometer technology are the lower bulk resistivity and superior resistance to electromigration as well as stress migration of Cu compared to Al and its alloys. However, many studies have suggested that the interaction of Cu and Si at moderate temperatures can cause integrated circuit device degradation. The reported failure mechanisms include the formation of decorating defects,[1] such as dislocation pipes, which cause the shorting of a p-n junction, the formation of silicides, which reduces the conductivity,[2,3] and the generation of donor or acceptor levels in Si bandgap,[4] which results in subthreshold shift and junction leakage in complementary metal oxide semiconductor devices. Research also shows that Cu diffuses rapidly in Si at modest temperatures[5] and in the presence of an electric field.[6] Therefore, a diffusion barrier is employed to retard the penetration of Cu into either Si or SiO_2

Overall requirements for diffusion barriers were summarized by Kattelus and Nicolet in 1989.[7] Several transition metals and their nitride films, such as Ta,[8,9] Ta_xN,[3,10,11] Ti_xN,[12] and W_xN[13] have been considered as potential candidates for a diffusion barrier in Cu metallization. Recently, Ta_xN has received increasing attention among researchers due to its high thermal stability and chemical inertness with Cu at elevated temperatures.[14] However, both Cu and Ta_xN diffusion barriers are subjected to various annealing treatments in O_2, N_2, and Ar at relatively high temperatures during backend processing. The stability of the Cu/Ta_xN metallization during annealing in the presence of such gases is not known. Since these treatments may influence the stability of the metallization, it is important to establish the effect of different annealing ambients on the integrity of the copper interconnect.

For an effective diffusion barrier, the step coverage, or conformity, is important for high-aspect-ratio vias and contact holes on the fabricated devices. In such cases, the method of deposition plays a significant role. In this study, thin $Ta_{2.3}N$ films were deposited by the ionized metal plasma (IMP) sputtering method. The step coverage of IMP $Ta_{2.3}N$ films is better than that of the films deposited by conventional sputtering methods due to enhanced directionality of the sputtered ions under the influence of an applied electrical potential from a radio frequency (rf) coil. Deposition of thin $Ta_{2.3}N$ by the IMP method can achieve a bottom coverage of about 40% and a sidewall coverage of about 29% of the top layer thickness. Thus, in the present work, Cu/IMP $Ta_{2.3}N$ metallization was used to study the effect of different gases on this integrity during annealing.

Experimental

Multilayer films consisting of Cu, ImP $Ta_{2.3}N$, and SiO_2 were deposited onto 8 in. diam p-type Si(100) wafers for this study. Prior to the deposition of any metal film, a layer of 4.7 kÅ plasma-enhanced chemical vapor deposited silicon oxide was deposited onto the Si substrate. The wafers were degassed, and the surfaces of the substrates were sputter-cleaned by Ar^+ bombardment for 30 s, which removed approximately 200 Å of oxide. $Ta_{2.3}N$ films about 35 nm thick were then deposited by the IMP sputtering method using a base pressure of 28 mTorr, an rf power of 1.5 kW, and a substrate bias of 350 W. During deposition, the substrate temperature was kept constant at 100°C. Subsequently, 55-60 nm thick Cu films were deposited onto $Ta_{2.3}N$ films without breaking the vacuum, using a long-throw configuration (γ-Cu) sputter deposition with an rf power of 2 kW. The chamber pressure during Cu deposition was 20 mTorr.

To elucidate the effects of the annealing ambient, three sets of Si/SiO_2/$Ta_{2.3}N$/Cu samples were annealed at temperatures ranging from 200 to 800°C for 30 min with a constant ramp rate of 5°C/min starting from room temperature (25°C). One set of samples was annealed in a N_2/O_2 mixture (~20% O_2), while the other two sets were annealed in purified Ar and N_2, respectively. The changes in electrical properties of the Cu/$Ta_{2.3}N$ metallization as a function of annealing temperature in different ambients were monitored using the four-point probe measurement technique. X-ray diffraction (XRD) and transmission electron microscopy (TEM) techniques were used to examine the texture and microstructure of the as-deposited films. XRD was carried out using a Philips X'PERT system equipped with a Cu Kα X-ray radiation operated at 45 keV and 40 mA. The composite films and the reactions between the films at different temperatures were studied by Rutherford backscattering spectrometry (RBS), Auger electron spectroscopy (AES), cross-sectional TEM (XTEM), scanning electron microscopy (SEM), and energy dispersive X-ray (EDX) techniques. The RBS analysis was carried out using a 2 MeV He^{2+} beam with a backscattered angle of 20°. The elemental composition of the tantalum nitride films was obtained from RBS data using standard RUMP analysis.

* Electrochemical Society Active Member.
z E-mail: yapkp@charteredsemi.com

S0013-4651(99)07-002-0 CCC: $7.00

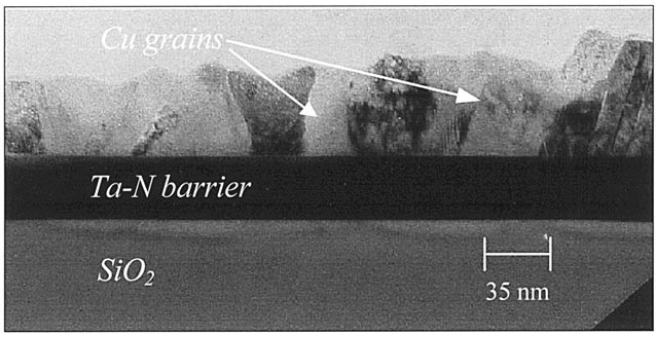

Figure 1. XTEM picture of an as-deposited sample showing smooth Cu/$Ta_{2.3}N$ and $Ta_{2.3}N/SiO_2$ interfaces.

Results and Discussion

Recrystallization of amorphous $Ta_{2.3}N$ film.—XTEM micrography shows that the as-deposited IMP $Ta_{2.3}N$ barrier layer is uniform and planar. As illustrated in Fig. 1, both the Cu/$Ta_{2.3}N$ and $Ta_{2.3}N/SiO_2$ interfaces are planar and smooth. There is no reaction or intermixing at these interfaces initially. Results from RBS compositional analysis suggest that the Ta:N ratio is about 2.3:1. Figure 2 shows the XTEM picture of the as-deposited IMP $Ta_{2.3}N$ sample. To obtain the diffraction pattern, the beam size used was 10-20 nm. The electron diffraction pattern obtained shows that this barrier layer is amorphous. The diffused nature of the pattern did not change significantly as the beam size was reduced from 20 to 10 nm. However, the film starts to recrystallize at 500°C in N_2 ambient. A typical TEM picture of a recrystallized $Ta_{2.3}N$ film is shown in Fig. 3. The lattice parameter of this film is 4.9 Å, which is in good agreement with the reported lattice constant *c* of the hexagonal Ta_2N. XRD results also support the above finding. As shown in Fig. 4, the XRD spectrum of the as-deposited barrier layer exhibits the characteristics of an amorphous material, which is in accordance with the TEM observation mentioned above. When the films are annealed to 500°C, sharp peaks appear at diffraction angles of 38.7, 50.9, 60.9, 67.5, 71.5, 73.1, 74.5, and 77.6, which correspond, respectively, to the (101), (102), (110), (103), (200), (112), (201), and (004) reflections of hexagonal Ta_2N. The Cu(220) peak intensity generally increased upon annealing, although the changes in the intensity were not systematic. Grain growth is a possibility that can account for these changes. However, in the present work, no detailed work was done using TEM to determine the effect of annealing on grain growth. Observation of the Cu film surface before the after annealing by SEM at a magnification of up to 5000 times did not reveal any significant changes in the surface features.

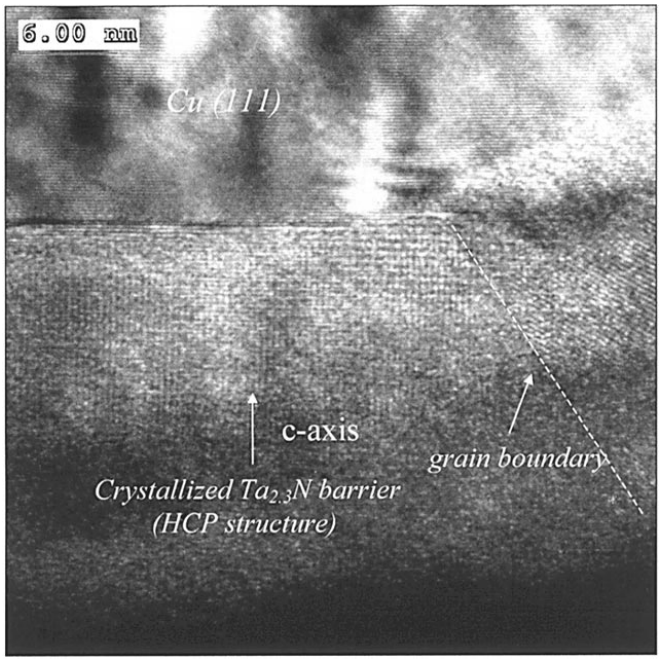

Figure 3. Interface between the Cu and recrystallized $Ta_{2.3}N$ barrier films. The lattice parameter *c* of the barrier is 4.9 Å.

Annealing in N_2/O_2 mixture.—To determine the change in electrical properties of the Cu/$Ta_{2.3}N$ metallization as a function of temperature and annealing ambient, the sheet resistances of the as-deposited and annealed samples were measured by the four-point probe technique. The variations in sheet resistance of sample annealed in N_2/O_2, Ar, and N_2 ambient at various temperatures are shown in Fig. 5. The average sheet resistance of the as-deposited Cu film is about 0.45 Ω/□, which corresponds to a resistivity of 2.5 μΩ/cm. The sheet

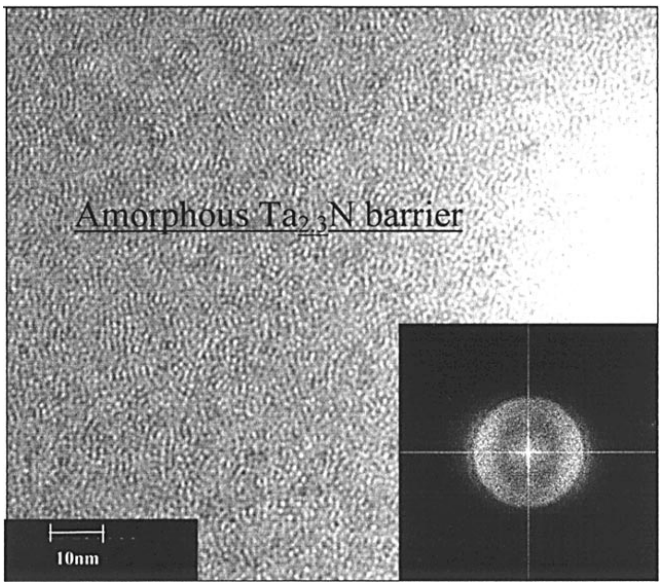

Figure 2. High resolution TEM picture and electron diffraction pattern of as-deposited IMP $Ta_{2.3}N$ film.

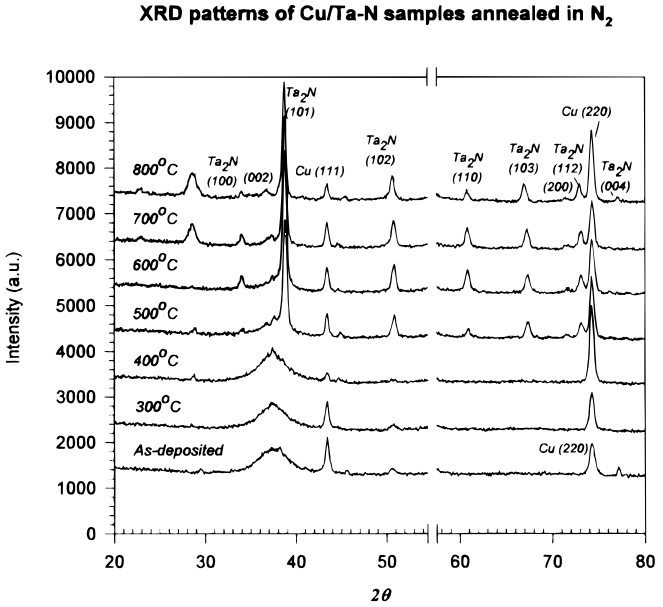

Figure 4. XRD pattern of the IMP $Ta_{2.3}N$ barrier layers before and after annealing in N_2 ambient.

S0013-4651(99)07-002-0 CCC: $7.00

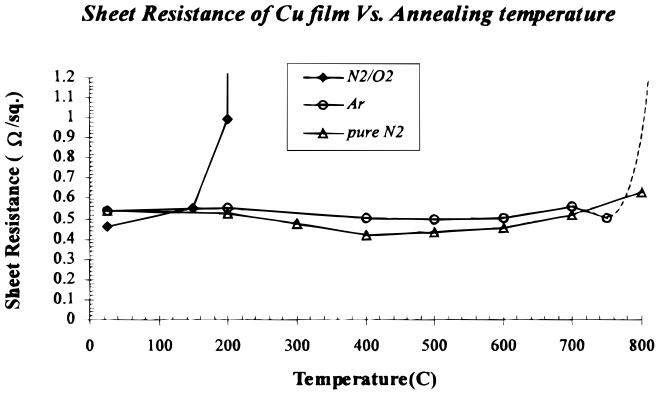

Figure 5. Variations in the sheet resistance of $Cu/Ta_{2.3}N/SiO_2/Si$ films in various annealing ambients as a function of annealing temperature.

resistance of the $Cu/Ta_{2.3}N$ films remains unchanged upon annealing in N_2/O_2 at 150°C However, as the annealing temperature is increased to 200°C, the sheet resistance increases by a factor of 2. The surface of the annealed sample appears to be hazy and becomes slightly reddish in color. At 300°C, the sheet resistance increases about ten times, and the surface becomes silvery. Assuming that the Cu film carries all the sensor current, this result indicates that the effective thickness of the Cu film is reduced to 1/10 of its original value. The multilayer films become completely insulating upon annealing at 500°C.

To further elucidate the effects of N_2/O_2 ambient on the $CuTa_{2.3}N$ films, RBS, AES, and TEM techniques were employed to investigate the $Cu/Ta_{2.3}N$ and $Ta_{2.3}N/SiO_2$ interfaces. Figure 6 shows the RBS spectra of $Cu/Ta_{2.3}N/SiO_2/Si$ samples before and after annealing in N_2/O_2 ambient. The Cu and Ta peaks of the as-deposited films are clearly separated, as shown in Fig. 6a. The energies of the leading and trailing edges of the Ta signal are around 1.765 and 1.699 MeV, respectively. Samples annealed at 200°C are found to exhibit two Ta peaks. The leading edge of the higher energy Ta peak is located at 1.808 MeV, and the maximum of this peak occurs at 1.777 MeV. This observation suggests either an out-diffusion of Ta into the Cu film or a reduction in the Cu film thickness. However, investigation using XTEM does not appear to indicate any appreciable diffusion or intermixing at $Cu/Ta_{2.3}N/SiO_2$ interfaces at this temperature (Fig. 7a). Thus, the observed Ta peaks seems to indicate the formation of voids in the Cu film resulting in the reduction of the Cu film thickness at the void regions. Since the energy at the leading edge of the Ta peak is less than the energy of the backscattered He^{2+} ions from a pure Ta sample surface (which is 1.836 MeV), the voids in the film are not through-holes. The depths of such voids are measured by atomic force microscopy (AFM) and are determined to be around 30 nm deep, which is less than the thickness of the Cu film (60 nm). Therefore, the higher energy Ta peak corresponds to the signal of He^{2+} ions backscattered from the $Ta_{2.3}N$ layer underneath the voids in the Cu film. From the ratio of the areas under the two Ta peaks, the area of $Ta_{2.3}N$ underneath the valids is calculated to be 64%. This value is in good agreement with the density of voids observed by SEM, as illustrated in Fig. 8a. In addition to the appearance of the higher energy Ta peak, there also is an observable upward shift of the Si signal. This again corresponds to the SiO_2 underneath the voids. At the same time, there is a change in the width of Cu peak, which indicates an increase in the thickness of the Cu layer. The signal of the trailing edge of the Cu peak shifts to a lower energy of 1.440 MeV. RBS simulation using RUMP analysis shows that a substantial amount of oxygen is present at the Cu surface. The simulation also suggests the formation of a Cu oxide layer about 32 nm thick. This explains the increase in the sheet resistance by a factor of 2 when the sample is annealed at 200°C, since the effective Cu thickness is reduced to about 30 nm due to the oxide formation. Incorporation of oxygen into Cu results in a decrease of the slope of the trailing edge of the Cu peak, as well as an increase in the Cu peak width. The composition of the oxide is determined to be Cu_2O from the simulation.

RBS spectra of samples annealed at 300, 400, and 500°C in N_2/O_2 are shown in Fig. 6b. In the first two spectra, the width of the Cu peak increases while the height decreases, indicating formation of Cu oxides. Since no separate Ta peak is observed, the Cu oxides formed at 300 and 400°C are expected to be free of voids. In addition, there is an increase in the thickness of the oxide layer formed at 400°C compared to 300°C, as evidenced by an increase in the Cu peak width and a downward shift in the location of the Ta peak. RUMP analysis of the RBS data shows that the oxide formed at 400°C is CuO. Examination of the XTEM photographs of the $Cu/Ta_{2.3}N$ interface shows that the Cu oxide layer begins to delaminate from the interface upon annealing at 400°C, as illustrated in Fig. 7b. Gaps are found between the Cu oxide and $Ta_{2.3}N$ barrier at some regions along the interface. However, the interface between the barrier and SiO_2 remains smooth and intact. Figure 6b also shows the

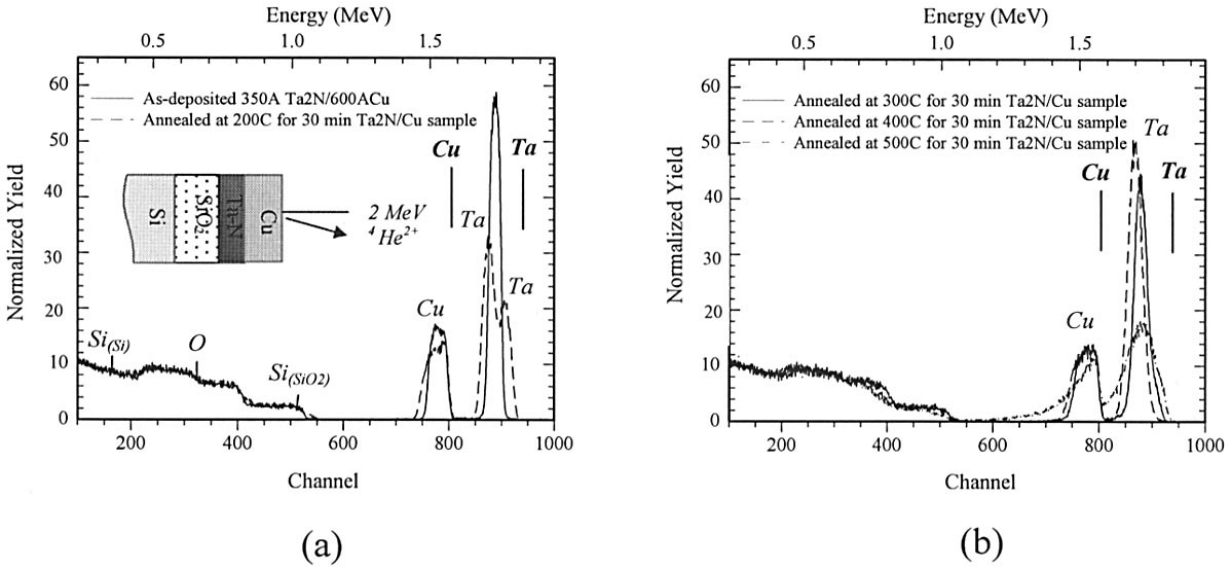

Figure 6. RBS spectra (2 MeV He^{2+}, $\theta = 0°$, $\phi = 20°$, $\varphi = 20°$) of $Cu/Ta_{2.3}N/SiO_2/Si$ films annealed in N_2/O_2. (a) As-deposited and annealed at 200°C; (b) annealed at 300, 400, and 500°C.

S0013-4651(99)07-002-0 CCC: $7.00

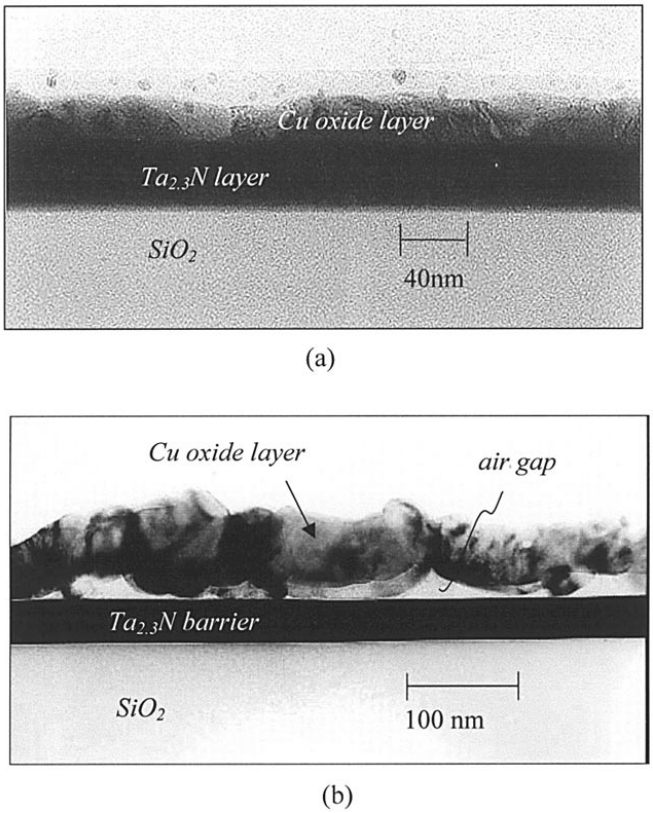

Figure 7. XTEM micrograph showing (a) no diffusion or intermixing at the two interfaces upon annealing at 200°C in N_2/O_2, and (b) delamination of Cu oxide film at CuO/$Ta_{2.3}N$ interface upon annealing at 400°C in N_2/O_2.

RBS spectrum from a sample annealed at 500°C. As is shown later, these annealed films are very rough. The observed RBS spectrum could be explained reasonably well, taking into consideration the roughness of the films.

As the results of RBS are greatly affected by the morphologies and interface roughness of the samples, they should be interpreted in conjunction with SEM and AFM photographs. SEM pictures of the annealed Cu film surfaces are shown in Fig. 8. Examination of the films annealed at 200°C by SEM and AFM shows that the surface is very rough and the films are porous, containing a large number of voids. The microstructure is similar to that observed in oxides formed on Cu lead-frames annealed in air at temperatures below 300°C.[15] The root-mean-square (rms) roughness of the sample annealed at 200°C is approximately two times the roughness of the as-deposited sample. Thus, it is likely that upon oxidation the thickness of the Cu and the Cu oxide over the $Ta_{2.3}N$ layer becomes nonuniform due to the roughness and presence of voids. This seems to explain the appearance of the higher energy Ta signal in the RBS spectrum for the sample annealed at 200°C.

The morphology of the Cu films annealed at 300 and 400°C is different from that of the sample annealed at 200°C. As shown in the SEM picture in Fig. 8c, the sample annealed at 400°C appears to be free of voids. The sample annealed at 300°C (Fig. 8b) shows some roughness, but does not seem to have any voids. The mechanisms of Cu film oxidation at low temperatures were studied by Li *et al.*[16] It was observed that Cu is first oxidized to Cu_2O at 200°C and then to CuO at 300°C. The oxidation starts at the copper surface and progresses slowly into the bulk. Since the inward diffusion of oxygen proceeds gradually as a function of annealing time, the complete oxidation from Cu_2O to CuO depends on the annealing condition. In the present experiment, the observed microstructure of the sample annealed at 300°C is likely the result of partial transformation of Cu_2O into CuO at the surface. The oxide layer appears to consist of CuO islands on the surface of the bulk Cu_2O layer. This is in accordance with the RBS simulation result indicating that the bulk of the oxide is Cu_2O. The observed roughness also explains the decrease in the gradient of the trailing edge of the Cu signal and the leading edge of the Ta signal (with respect to the as-deposited sample) in the RBS spectra.

Annealing at 400°C results in the formation of mainly CuO, as indicated by RBS analysis. Analysis of the electron diffraction pattern (Fig. 8d) from the oxide also shows that the oxide is CuO. RBS data indicates an increase in film thickness, as expected from the conversion of Cu into CuO. Both SEM and AFM observations indicate that the surface of the oxidized films is relatively smooth. As the annealing temperature is increased to 500°C, film roughness increases greatly, by more than 10 times, as shown in Fig. 8e.

Annealing in purified Ar.—Variations in the sheet resistance as a function of annealing temperatures in an Ar ambient are illustrated in Fig. 5. The sheet resistance remains unchanged even after annealing at 750°C. However, as the temperature is increased beyond 750°C, the sheet resistance increases by several orders of magnitude. The drastic increase of the sheet resistance suggests the degradation of the Cu/$Ta_{2.3}N$ interconnect system.

To investigate the reason for the change in sheet resistance, the RBS technique was employed. RBS spectra of sample annealed in Ar ambient are shown in Fig. 9. It is observed that the spectra from samples annealed below 600°C (Fig. 9a) are similar to that of the as-deposited sample, indicating that the integrity of this interconnect remains unchanged. However, for an annealing temperature of 600°C and above, a small Ta peak is observed at the higher energy of 1.836 MeV (Fig. 9b), which corresponds to the energy of pure Ta on the surface. This indicates diffusion and accumulation of a small amount of Ta at the top surface of the sample. As the temperature is increased further to 750°C, the amount of Ta accumulated at the surface increases. RBS simulation suggests that the small Ta peak corresponds to only a few monolayers of Ta, which implies that the small Ta peak is not from any exposed barrier layer. However, the interface between $Ta_{2.3}N$ and SiO_2 remains smooth and intact at 750°C, as shown in Fig. 10. Complete failure of Cu/$Ta_{2.3}N$ metallization occurs upon annealing at 800°C in Ar. RBS data suggest that the intermixing of all elements occurs at 800°C, as indicated by the appearance of new peaks of Cu, Ta, and Si.

To complement the RBS results, samples annealed at 500, 600, 750, and 800°C in Ar were investigated by SEM also. Surface morphologies of the samples annealed below and at 600°C are essentially the same as that of the as-deposited sample. Upon annealing the sample above 600°C, hillock formation was observed at the surface, as shown in Fig. 11a. The density of hillocks upon annealing at 750°C was 0.26 hillocks/μm^2. The composition of the hillocks with diameters greater than 1 μm was determined by EDX and AES. The presence of only Cu is detected in these hillocks. However, AES analysis of the surface without any hillocks (spot 1 in Fig. 11a) indicates the presence of no other element but Cu. However, as earlier noted, RBS measurements indicate out-diffusion of Ta to the Cu surface. This is attributed to local diffusion of Ta through defects, such as grain boundaries. Upon annealing at 800°C formation of a large concentration of hillock-like structures is observed (Fig. 11b). These structures occupy approximately 50% of the total surface areas. Examination of the surfaces of these hillock-like structures and the remaining film by AES indicates the presence of Cu, Ta, Si, and O everywhere. For examples, the analysis of spot 1 and spot 2 in Fig. 11b shows the compositions (in atomic percentage) as 21% Cu, 14% Ta, 41% Si, 25% O, and 3% Cu, 5% Ta, 58% Si, and 34% O, respectively. This is indicative of complete intermixing of the elements by diffusion and substantial agglomeration of the Cu film.

Annealing in purified N_2.—Variations in the sheet resistance of samples annealed in N_2 as a function of annealing temperatures are shown in Fig. 5. It is observed that the sheet resistance remains unchanged (at 0.5 Ω/□) on annealing to 800°C.

RBS spectra of samples annealed in the N_2 ambient are shown in Fig. 12. As shown in Fig. 12a, the location and shape of the Cu, Ta,

S0013-4651(99)07-002-0 CCC: $7.00

and Si peaks for samples subjected to 200, 300, and 400°C annealing are essentially the same as those of the as-deposited sample, indicating that the integrity of this interconnect remains unchanged. However, when the sample was annealed at 500°C, the leading edge of Ta signal extended to a higher energy of 1.829 MeV (Fig. 12b), indicating the diffusion of a small amount of Ta into Cu. Nevertheless, the Cu surface seems to be free of Ta, since the energy of this Ta peak is less than the energy of the backscattered He^{2+} ions from the surface of a pure Ta sampler. It seems that the outdiffused Ta atoms remain mainly distributed within the Cu film grain boundaries. However, the sample annealed at 600°C exhibits a Ta peak at an energy of 1.836 MeV, which corresponds to a few monolayers of Ta at the Cu film surface. As the annealing temperature is increased to 700 and 800°C, the height of this Ta peak increases. In addition, a gradual decrease in the gradient of the leading edge of the lower energy Ta peak also is observed. These observations indicate a gradual diffusion of Ta into Cu and accumulation at the Cu surface upon annealing around 600°C and above.

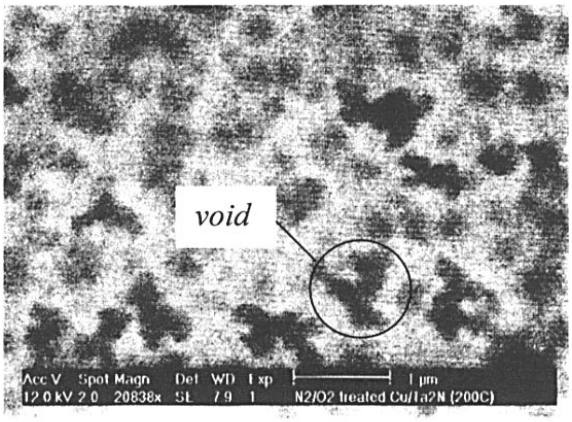

(a)

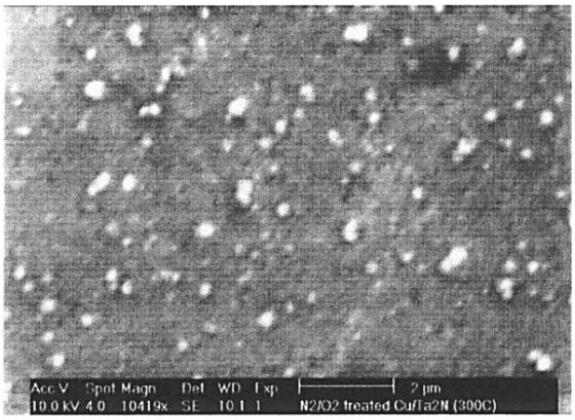

(b)

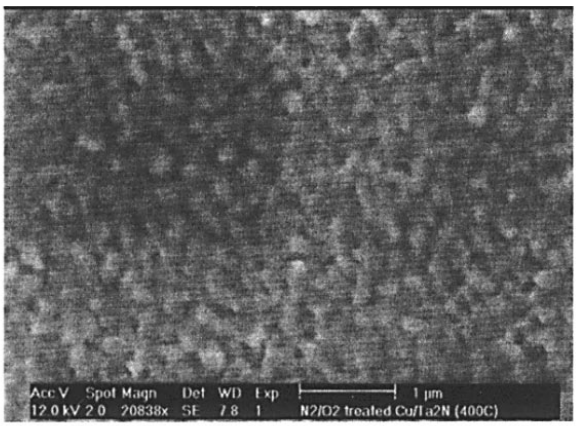

(c)

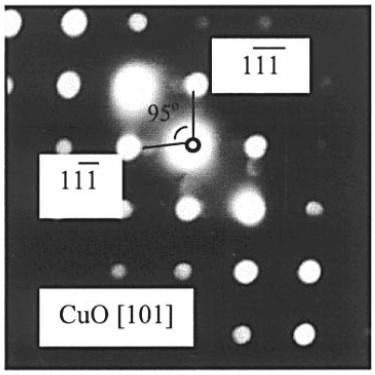

(d)

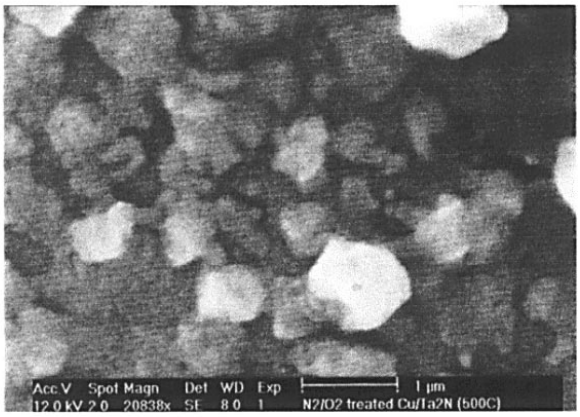

(e)

Figure 8. SEM pictures showing the surfaces of the samples annealed in N_2/O_2 for 30 min at (a) 200, (b) 300, (c) 400, and (e) 500°C. (d) shows the electron diffraction pattern from the film shown in (c).

S0013-4651(99)07-002-0 CCC: $7.00

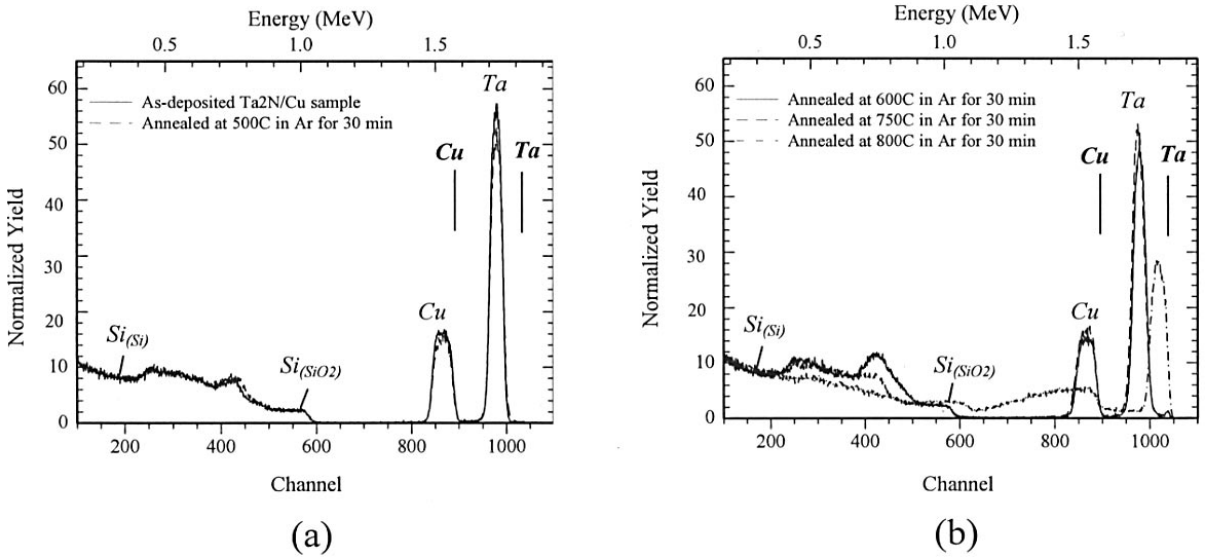

Figure 9. RBS spectra (2 MeV He^{2+}, $\theta = 0°$, $\phi = 20°$, $\varphi = 20°$) of $Cu/Ta_{2.3}N/SiO_2/Si$ films annealed in Ar. (a) As-deposited and annealed at 500°C; (b) annealed at 600, 750, and 800°C.

Conclusions

The effects of the annealing ambient on the integrity of $Cu/Ta_{2.3}N$ metallization have been investigated using four-point probe, RBS, XTEM, AES, SEM, AFM, and EDX techniques. It is observed that in the presence of N_2/O_2, the integrity of the $Cu/Ta_{2.3}N$ interconnect begins to degrade significantly at an annealing temperature of 200°C, which is attributed to the formation of Cu oxide with a high density of voids. Annealing of the interconnect at 400°C results in delamination of the Cu oxide/$Ta_{2.3}N$ interface. The sheet resistance increases drastically upon annealing above 200°C. In an Ar or N_2 annealing ambient, the integrity of the $Cu/Ta_{2.3}N$ metallization remains essentially unchanged up to about 500°C. Diffusion of Ta into the Cu films seems to start along grain boundaries in the range of ~500 to 600°C. Annealing to higher temperatures results in accumulation of Ta on the surface of the Cu films. However, the sheet resistance of the metallization remains unchanged if the annealing temperature does not exceed 750°C. The result demonstrates that the integrity of Cu metallization with $Ta_{2.3}N$ diffusion barriers depends significantly on the annealing ambient. It is important to isolate the $Cu/Ta_{2.3}N$ metallization from oxygen exposure during backened processing.

Acknowledgments

The authors thank Applied Materials for their support in sample preparation. The authors also acknowledge D. Mangelinck for support and valuable discussion on RBS analysis. The authors are grateful to K. C. Toh and Y. Wang for their technical assistance on the XRD experiment.

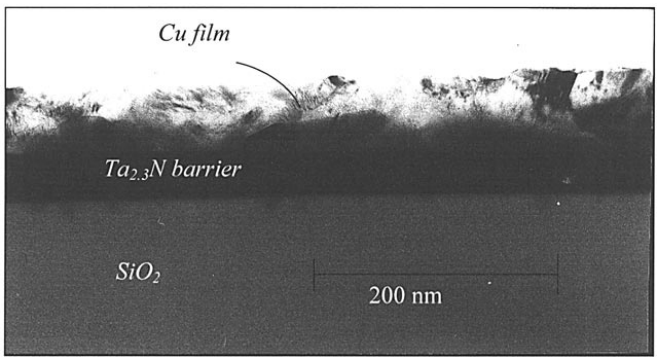

Figure 10. XTEM micrograph showing smooth and intact $Ta_{2.3}N/SiO_2$ interface upon annealing at 750°C in Ar.

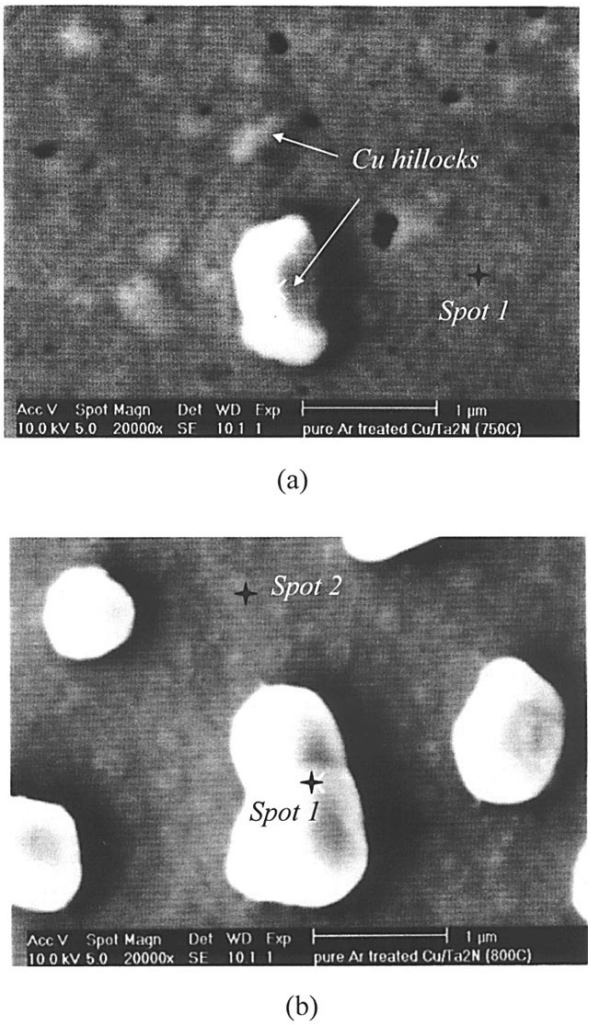

Figure 11. SEM micrographs showing the morphologies of the samples annealed in Ar at (a) 750 and (b) 800°C.

S0013-4651(99)07-002-0 CCC: $7.00

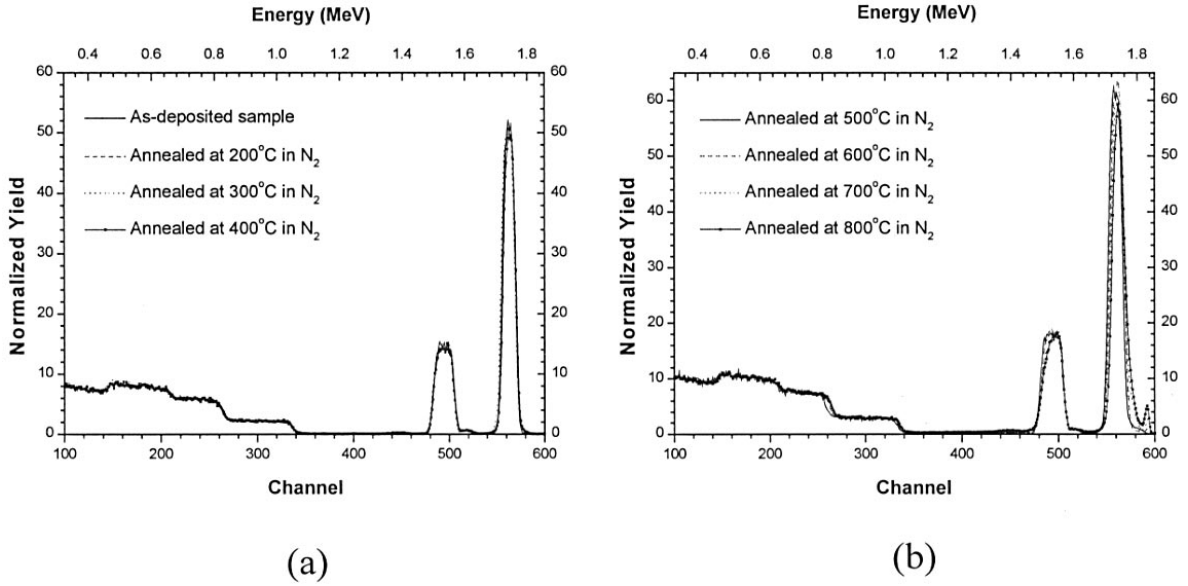

Figure 12. RBS spectra (2 MeV He^{2+}, $\theta = 0°$, $\phi = 20°$, $\varphi = 20°$) of $Cu/Ta_{2.3}N/SiO_2/Si$ films annealed in N_2. (a) As-deposited and annealed at 200, 300, and 400°C; (b) annealed at 500, 600, 700, and 800°C.

National University of Singapore assisted in meeting the publication costs of this article.

References

1. R. D. Thompson and K. N. Tu, *Appl. Phys. Lett.*, **41,** 440 (1982).
2. M. Setton, J. Van der Spiegel, and B. Rothman, *Appl. Phys. Lett.*, **57,** 357 (1990).
3. K. Holloway, P. M. Fryer, C. Cabral, J. M. E. Harper, P. J. Bailey, and K. H. Kelleher, *J. Appl. Phys.*, **71,** 5433 (1992).
4. A. G. Milnes, *Deep Impurities in Semiconductors*, Wiley, New York (1973).
5. E. R. Weber, *Appl. Phys. A*, **30,** 1 (1983).
6. J. D. McBrayer, R. M. Swanson, and T. W. Sigmon, *J. Electrochem. Soc.*, **133,** 1243 (1986).
7. H. P. Kattelus and M.-A. Nicolet, in *Diffusion Phenomena in Thin Films and Microelectronic Materials*, D. Gupta and P. S. Ho, Editors, p. 432, Noyes, Park Ridge, NJ (1989).
8. E. Kowala, J. S. Chen, J. S. Reid, P. J. Pokela, and M.-A. Nicolet, *J. Appl. Phys.*, **70,** 1369 (1991).
9. K. Holloway and P. M. Fryer, *Appl. Phys. Lett.*, **57,** 1736 (1990).
10. K.-H. Min, K.-C. Chun, and K.-B. Kim, *J. Vac. Sci. Technol. B*, **14,** 3263 (1996).
11. J.-C. Lin and C. Lee, *Electrochem. Solid-State Lett.*, **2,** 181 (1999).
12. J. O. Olowolfe, J. Li, and J. W. Mayer, *Appl. Phys. Lett.*, **58,** 469 (1991).
13. M. Uekubo, T. Oku, K. Nii, M. Murakami, K. Takahiro, S. Yamaguchi, T. Nakano, and T. Ohta, *Thin Solid Films*, **286,** 170 (1996).
14. T. Oku, E. Kawasaki, M. Uekubo, K. Takahiro, S. Yamaguchi, and M. Murakami, *Appl. Surf. Sci.*, **99,** 265 (1996).
15. S. K. Lahiri, N. K. Waalib Singh, K. W. Heng, L. Ang, and L. C. Goh, *Microelectron. J.*, **29,** 335 (1998).
16. J. Li, J. W. Mayer, and E. G. Colgan, *J. Appl. Phys.*, **70,** 2820 (1991).